Electrodynamic withstand and effects of short-circuit currents on high-voltage electrical equipment

Alexander Khrennikov [1]*, *Robert* Shulga[2], and *Nikolay* Alexandrov[3]

[1]JSC "STC FGC UES" Rosseti, 123007 Kashirskoe Highway, 22, Moscow, Russia
[2]VEI-branch of FSUE " RFNC-VNIITF im. Akademik E. I. Zababakhina", 105118 Krasnokazarmennaya st., 12/38, Moscow, Russia
[3]SPE Dynamics, 428000 Anisimova str, 6, Cheboksary, Russia

Abstract. The analysis of simplified expressions allows us to estimate the electrodynamic effects of short-circuit currents on the main elements of a power electrical station and substation, which include busbars, high voltage circuit-breakers, disconnectors, electrical machines and transformers. Examples of calculations of magnetic field induction, mechanical forces and pressures that determine the electrodynamic withstand of electrical equipment are given. Simplified qualitative calculations allow us to assess the impact of key parameters on the selection of appropriate elements and the possible range of their changes during the design, operation and modernization at the preliminary design stage.

1 Introduction

The mechanical effects of short-circuit currents (SC) determine the resistance of electrical equipment to electrodynamic influences. The power electrical circuit of electric power station and substation contains electrical machines (EM) in the form of a generator or motor, a busbar, high voltage circuit-breakers (CB) and a disconnector, a power transformer and an overhead transmission line or cable line. Transient processes in these elements are quite widely described in the literature, for example, in [1, 2] for EM, in [3,4] for power transformer, and the calculated modes of switching on and short-circuit are given in [5,6].

Currently, there is a modernization and improvement of electrical equipment to improve energy efficiency through the use of new designs, technologies and materials [6 - 8].

Despite the availability of digital programs for calculating overcurrents and mechanical effects, for example, EMTP, ETAP, REST, ELAX - 2D, ELINDST 2.0, etc., there is a need to conduct high-quality calculations of the rigidity and stability of transformer windings during short-circuit: calculation of the magnetic field, strength of winding conductors during bending by axial and radial forces, axial vibrations of transformer windings, allowable electric field strengths of oil barrier insulation, value of insulation safety factors.

Block diagram of the connections of power elements at electric power station or substation shows on fig. 1, where they are indicated: EM - electric machine, busbar, CB - high voltage circuit-breaker and D - disconnector, T - power transformer, L - overhead transmission (cable) line.

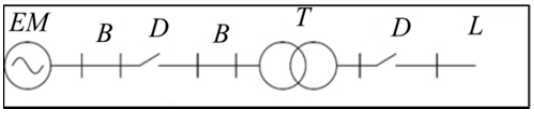

Fig. 1. Block diagram of the connections of power elements at electric power station or substation.

2 BUSBAR

When calculating the strength of execution and termination on busbar insulators (W), in accordance with Ampère's law, the magnetic induction B is determined by the formula

$$B = \mu_0 I / 2\pi d, \quad (1)$$

where $\mu 0 = 4\pi \times 10\text{-}7$ *H/m*, *I*, *d* are respectively the amplitude of the current and the distance between the busbars, *l* is the length of the busbar.

In the case of the opposite direction of current *I* in two parallel busbar trunkings of length *l* , repulsive forces *F* arise, which are equal to

$$F = 2 \times 10^{-7} \times I2 \times l/d \quad (2)$$

Figure 2a shows the arrangement of 2 parallel busbars, and fig. 2b shows the vectors of currents *I*, magnetic inductions *B*, and repulsive forces *F*.

* Corresponding author: ak2390@inbox.ru

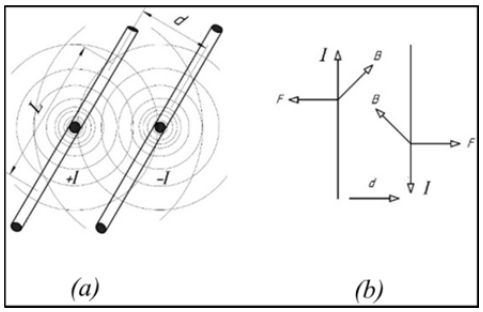

Fig. 2. Arrangement of parallel busbars with current *I* of length *l* (a) and vectors of counter currents *I*, magnetic inductions *B* and repulsive forces *F* (b).

Example 1. Given the values of the short-circuit current equal to $I=10^5$ *A*, *d*=0.5 *m*, = 1 *m*, in accordance with (2) the value *F*=4000 *N* or 400 *kg* of force that the switchgear busbars must withstand at a length of 1 m.

Example 2. For a test circuit with a tubular busbar for a 1200 MW turbo generator of Nuclear Power Station with a short-circuit current of 300 kA at a distance of *d* = 5 m, the repulsive force is 3600 N over a length of 1 m.

When exposed to a sinusoid of short-circuit current with amplitude I_k, dissipation factor σ, mains frequency ω, attenuation coefficient α in formula (2), the value of I_2 should be taken equal to

$$I_2 = I_K^2/\sigma(\cos(\omega t)- e^{-\alpha t})2= \\ =(I_s/2)^2(1/2+e^{-2\alpha t}-2e^{-\alpha t}\cos(\omega t)+1/2\cos(2\omega t)) \quad (3)$$

As a result, the short-circuit current leads to the appearance of three components of mechanical effects: a constant force and two variable forces with frequencies that are multiples of ω and 2ω. When switching on the EM and power transformer, due to the asymmetric turn-on current, the current contains frequencies that are multiples of 1, 3, 5 harmonics.

3 Circuit-breaker (disconnector).

The equivalent circuit of the circuit breaker and disconnector (CB and D, respectively) is shown in Fig. 3,a. Due to the flow of current I in opposite directions of the horizontal branches, repulsive forces F arise between them. The same force causes the knives CB and D to separate from the traverse. Figure 3 shows the directions of the forces of interaction F in the circuit breaker and disconnector along the gap *x* of length *d*, the radius of the conductors and connections is *r*.

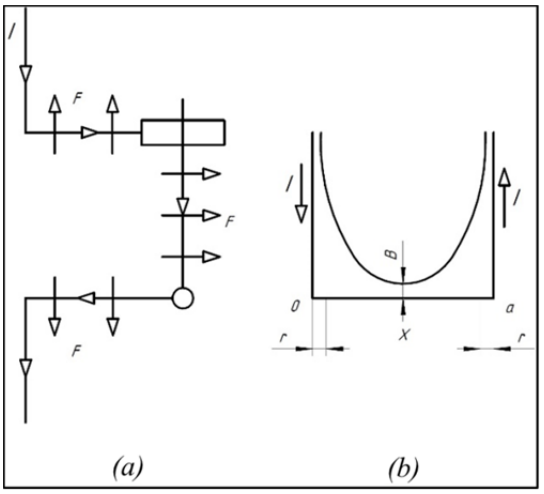

Fig. 3. Directions of interaction forces F in the circuit breaker and disconnector: a) interaction scheme of *F*, b) distribution of induction *B* (Tl) over the gap x of length *l*.

The force of interaction F for circuit breaker (disconnector) is determined

$$F = 2\cdot 10^{-7}\ \ln\left(\frac{d}{r}-1\right)\cdot I \quad (4)$$

Example 3. Given the values of the short-circuit current equal to $I=10^5$ A, *d* = 0.3 m, *r*= 0.01 m, *l* =1m, in accordance with (4) $F=2\times10^{-7}\ln(0.3 / 0.01^{-1})\times10^{10}$ = 6870 N, which is more than 1.5 times the impact force of Example 1 for parallel busbars.

4 Single-layer winding of an electrical machine.

The layout of conductors in a single-layer winding of electric machine is shown in fig. 4, where *l* is the length of the conductor, *x* is the current length of the EM slot, A is the linear current density (A/m).

On fig. 4b shows the case when the direction of induction B is perpendicular to the plane l_x.

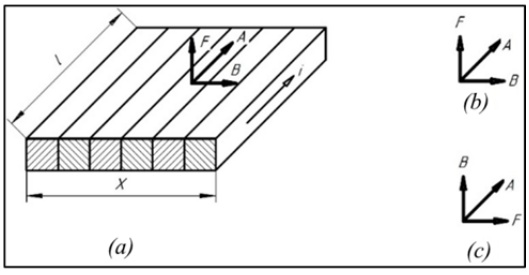

Fig. 4. Layout of conductors in a single-layer winding of electric machine (a), vectors of induction *B*, force *F* and linear current density *A* (b, c).

Linear current density A is

$$A = \sum I/x \ , \text{A/m} \quad (5)$$

The force of interaction of the magnetic field on conductors with current is

$$F = 10^{-6}\ \text{BA}\ lx\ , \text{N} \quad (6)$$

The specific pressure p per unit area *l* x is equal to

$$p = 10^{-6}\text{BA}\ \ \text{N/m}^2 \quad (7)$$

The effect of force on the windings of EM and power transformer from the magnetic field should be considered using the example of a power transformer.

5 Windings of the power transformer

The distribution of the magnetic field of induction B in the channel between the cylindrical windings of the power transformer is shown in fig. 5a. Ampère's law to the elementary circuit Adx in fig. 5a has the form of a circular integral

$$\int Hdx = Bdx = 4\pi Adx, \quad (8)$$

where linear current density $A = \sum I/x$ (A/m).

Neglecting the terms to the other three sides of the closed contour Adx, one can obtain

$$B_0 = 4\pi A \quad (9)$$

The distribution of induction B over the thickness of the winding is shown as a trapezoid in the lower part of fig. 5a.

The magnetic flux B, crossing the conductors in the axial direction, acts on the tension (expansion) of the winding outward (due to the opposite signs of the current and the linear current density A).

The average induction due to the trapezoidal distribution of B is B0/2. The radial pressure (force) pr from the axial component Bo is directed outward of the winding and is equal to

$$p_r = 10^{-7}\, 4\pi A_a^2, \quad (10),$$

where $A_a = \sqrt{2}\, A$.

When a short-circuit current flows through the transformer, the inner winding is subjected to a compressive force due to the direction of forces inward towards the magnetic core, and the outer winding experiences a tensile stress due to outward forces [5].

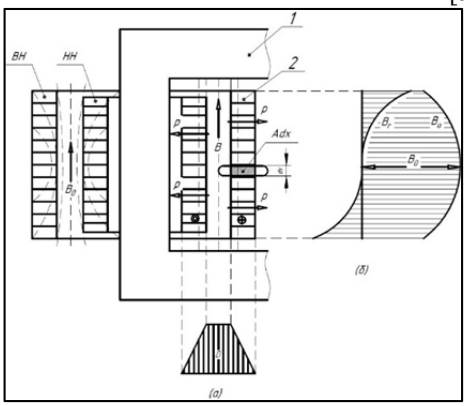

Fig. 5. The magnetic field of induction B in power transformer channel (a) and the components of the magnetic induction: B_r-radial, creates pressure pa, B_a-axial, creates pressure p_r (b); 1-core, 2- HV and LV windings.

Typically, tensile stress does not pose a risk of damage to the outer winding [2, 5]. The compressive stress of the radial forces causes damage to the internal winding - a wave of radial deformations (hoop buckling) (Fig. 6) [6 - 8].

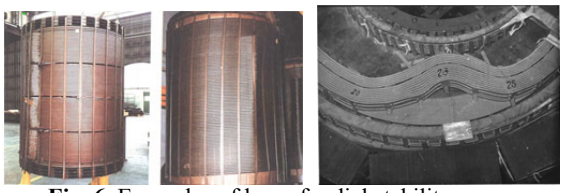

Fig. 6. Examples of loss of radial stability

6 Mathematical model of winding radial buckling

Next, a mathematical model is given for the radial deformation (example in the fig. 6) of one turn of a transformer winding in the form of an equation, which is more accurate than the previously presented models. Due to the use of trigonometric functions when describing the shape and volume of deformation and smaller error, this model more realistically reflects the processes occurring in the windings of power transformers in the case of short circuit.

Assumptions adopted in the preparation of the model:

The maximum size of the bulge of transformer winding is taken equal to the size of the concavity: a;

2. The convexity range is assumed to be equal to the concavity range: $\angle \Phi / 2$;

As an equation describing the concave-convex deformation of the current-conducting coil turn, the function $\varepsilon(\phi)$, described in polar coordinates, is chosen (Fig. 7):

$$\varepsilon(\phi) = a \cdot sin(2 \cdot \pi \cdot \phi / \Phi), with\ 0 \leq \phi < \Phi, \quad (11)$$

where a - maximum deformation, the maximum deviation of the distorted section from the ideal state;

$\angle\Phi$ - deformation range, the central angle within which the deformation is observed;

ϕ - is the function argument, the angle that is set clockwise from the vertical semiaxis.

The equation of radial deformation:

$$e(\phi) = a * sin(2 * \pi * \phi/\Phi), with\ 0 \leq \phi < \Phi. \quad (12)$$

The equation describing the shape of the turn of coil:

$$r(\phi) = R + e(\phi) = R + a * sin(2 * \pi * \phi/\Phi), with\ 0 \leq \phi < \Phi; \quad (13)$$

R - winding radius, with $\Phi \leq \phi < 2 * \pi$

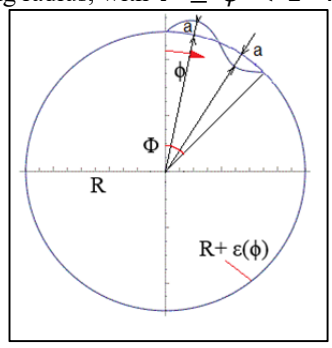

Fig. 7. Top view of the cylindrical winding of a power transformer with a concave-convex deformation after short-circuit with radial buckling.

The expression for the radial concave-convex deformation (11), for reasons of changing the position of the middle of the gap between the windings, we have for radial force:

$$F_r = \frac{\mu_0 (I_{max}\omega)^2 \rho_1 \pi (D_{12} + a \cdot \sin(2\pi\phi/\Phi)}{2h} \quad (14)$$

where μ_0 - is magnetic conductivity;

I_{max} - short circuit current amplitude;

ω - the number of turns of the winding through which short-circuit current flows;

ρ1 - the coefficient of reduction of the ideal leakage field to the real (Rogowski coefficient);

$D12$ - the distance of the tank wall to the middle of the gap between the windings;

h - winding height.

Φ - deformation range, the central angle within which the deformation is observed;

ϕ - is the function argument, the angle that is set clockwise from the vertical semiaxis.

The expression (14) for the radial force acting on the transformer windings in the event of a radial hoop buckling in case of a short circuit has greater accuracy than other expressions.

This expression (14) for the radial force more accurately reflects the processes occurring in the windings of power transformers in case of short circuit and the occurrence of radial hoop buckling, due to the use of trigonometric functions in describing the shape and volume of deformation, Φ - deformation range, the central angle within which the deformation is observed, and h - winding height [24-30].

7 Axial deformations and axial forces

An example of the axial deformation of the LV winding of 250MVA/220 kV transformer, i.e. the movement of the winding in the axial (vertical) direction under the action of electrodynamic forces during the flow of short-circuit currents (Fig. 8) [31-33].

Axial forces tend to bend the turns of the coils towards each other, which leads to the effect of tensile forces on the insulation layers between the turns of the inner and outer windings [5, 8]. Axial forces also exert pressure on the insulation of the winding concentrator. The change in short-circuit impedance in the HV-LV mode was Δ Zk = + 20% [7, 8].

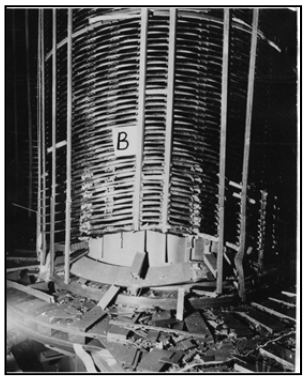

Fig. 8. Photo of phase "B" of the low voltage winding of 250MVA / 220 kV transformer, illustrating the loss of the axial stability of the winding, i.e. the movement of the winding in the axial (vertical) direction under the action of electrodynamic forces during the flow of short-circuit currents.

Own axial forces F_b (in newton) acting on the windings tend to reduce the height of the windings, therefore, the derivative of the magnetic field energy must be taken along the height of the winding h, i.e.

$$F_{b(2)} = \frac{\partial W_M}{\partial h} = \frac{1}{2} I_{max}^2 \frac{\partial L_k}{\partial h} = -\frac{\mu_0 (I_{max}\omega)^2 \rho_1 \pi D_{12} \delta'}{2h^2} \quad (15)$$

where $F_{b(2)}$ - own axial force acting on both windings.

If we consider the axial deformation as a change in the height of the winding, then the axial deformation formula will look like:

$$\Delta = h_{HV} - h_{LV}. \quad (16)$$

It follows that:

$$h_{HV} = h_{LV} + \Delta \quad (17)$$

Calculation of internal axial forces acting on the windings of the transformer is presented in fig. 9.

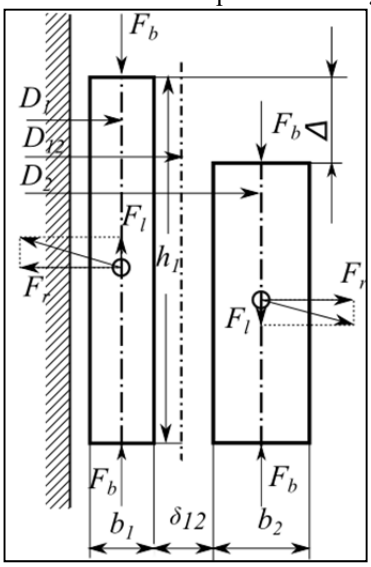

Fig. 9. Calculation of internal axial forces acting on the windings of the transformer.

You can substitute (17) in the formula (16) and then we get the expression for the axial force acting on the winding of the power transformer:

$$F_{axial} = -\frac{\mu_0 (I_{max}\omega)^2 \rho_1 \pi D_{12} \delta/}{2(h_{LV}+\Delta)} \quad (18)$$

Where $\delta' = \delta_{12} + \frac{b_1+b_2}{3}$, this is the maximum width of the main leakage channel.

8 Elliptical deformation of winding.

Here we study the case where one or more winding segments have been slightly deformed from the ideal circular form to an elliptic form [by 11] (Fig. 10).

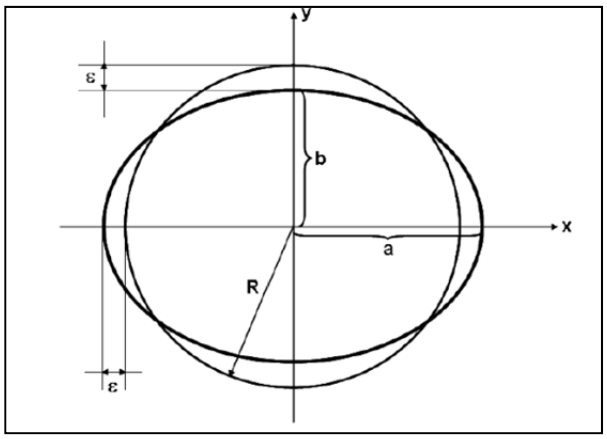

Fig. 10. Elliptical deformation.

To the first order of approximation in the small parameter ε/R, we obtain the following radial deformation $\delta\,(r,\varphi)$ of the elliptic winding compared to the unperturbed circular winding:

$$\delta(r,\varphi) = \delta(\varphi) = r - R = \varepsilon\, cos\,(2\varphi) \quad (19)$$

where R - the radius of the undeformed winding, r - the curve describing the elliptical deformation, ε=R-r(90°).

For small values of the ratio ε / R, the condition of maintaining the length of the coil before and after deformation is satisfied:

$$l = 2\pi R(1 + \varepsilon^2/(4R^2)) \approx 2\pi R \quad (20)$$

Substituting the equation of elliptic deformation into the force formula for radial deformation, we get:

$$F_r = (\mu_0\,(I_{max}\,\omega)^2\,\rho_1\,\pi(D_{12} + \varepsilon \cdot cos(2\varphi)))/2h \quad (21)$$

The whole refinement of the formula for radial forces is reduced to the fact that the distance D12 changes, which is the middle between the primary and secondary windings. Initially, we assume that only one of the windings is deformed, and then the formula correctly reflects the processes occurring in the transformer winding. In the literature about the second winding in the elliptical deformation is not mentioned.

The second assumption with elliptical deformation is that we mean that the ellipse is as the y axis perpendicular to the tank wall, but this may not be the case and will have to enter another angle into the equation. But this is a topic for further research.

9 Residual deformations with twisting of the winding and lodging of the turns on the edge.

Example 4. Setting for a powerful transformer by (4) with a normal linear current density *A*=75000 A/m and a short-circuit current equal to 20 *Inom*. (nominal current), the radial force is equal to p_r= 10-7×4π×(75000×20)2 =28260 N/m2

Example 5. For a power transformer with a power of 30,000 kVA, we take the following values (4):

a=1.25 m, b=0.04 m, c=1.3 m, d=0.1 m, A=75000 A/m, Ik=20×Inom., value of ln(a/b ×d/c) is 0.875. Then the axial force will be

p_a = 4×10-7×(75000 ×20)2 ×0.875 = 8000 N/m2 or 8 kg/cm2

As a result, the axial force is 4 times lower than the radial force. Axial forces from winding layers add up to the middle of the winding and can reach hundreds of tons. As long as the ratios a/b and c/d are almost equal, the axial forces remain acceptable. If the ends of one winding protrude relative to each other, then logarithm ln of these ratios increases sharply, and with it the axial force increases sharply.

It is also possible the occurrence of tangential winding twisting forces under the action of axial forces, which are much greater in the LV winding than in the HV. At a 500 kV substation, the autotransformer 250 MVA/500 kV/110 kV was disconnected from the action of gas protection. There were deformations of the HV winding with twisting and lodging of the turns on the edge under the action of tangential forces (Fig. 11) [6-8].

Fig. 11. Residual deformations of the HV winding of 250 MVA/500 kV/110 kV autotransformer with twisting of the winding and lodging of the turns on the edge.

10 220 kV SF_6 power transformer.

220 kV SF6 power transformer, produced by Russian Federation manufacturer, with a capacity of 63 MVA is a group of three single-phase 220 kV transformers with SF_6 insulation and cooling for normal operation, outdoor installation and at an underground substation is showed at fig. 12.

The design of the main units is determined: the core, the LV, HV and regulating windings, the LV, HV and regulating taps, the active part, the transformer tank and the on-load tap-changer.

The following calculations were carried out: electromagnetic calculation, insulation calculation, calculation of the electrodynamic withstand of

windings in case of short-circuit, gas-dynamic calculation of the cooling system, thermal calculation of the windings and magnetic system, calculation of the transformer tank and the tap changer tank for mechanical strength [9].

Fig. 12. 63 MVA/220 kV SF6 power transformer, produced by Russian Federation manufacturer.

Critical conductor subsidence forces, maximum axial forces and compressive stresses in spacers, average areas of insulation elements over which axial forces are distributed, and coefficients of rigidity of secant concenters were calculated using the ELDINST-2.0 program [9-12].

11 Conclusions.

1. Calculations of the mechanical impact of short-circuit current on high voltage circuit-breakers, disconnectors, electrical machines and power transformers, calculations of magnetic field induction, mechanical forces are given.

2. Received and investigated mathematical models: radial, elliptical, axial deformation of power transformer windings.

3. Calculations of the electrodynamic stability of the windings of SF_6 gas-insulated transformer 63 MVA/220 kV, produced by Russian Federation manufacturer, are given.

References

1. R. Ryudenberg, *Transient processes in electric power systems*, Moscow,712 p. (1955)
2. *Power transformers*. Reference book / Edited by S. D. Lizunov, A. K. Lokhanin. Moscow: Energoizdat, 616 p. (2004)
3. S. I. Lur'e *Stability of transformers during short circuit*. Moscow: Znak, 520 p. (2005)
4. R. N. Shulga, *Turn-on currents, short-circuit currents of transformers and synchronous generator*s, Energoekspert No. 2, pp. 44-48. (2021)
5. S.B. Vasyutinskiy, *Calculation and design of transformers*. Leningrad: LPI (1976)
6. A.Yu. Khrennikov, *High-voltage equipment in electrical systems: diagnostics, defects, damageability, monitoring*: textbook, Moscow: INFRA-M, 186 p. (2019)
7. A.Yu. Khrennikov, *Technical diagnostics and accident rate of electrical equipment*, Moscow: LITRES, 306 p. (2021)
8. A. Yu. Khrennikov, V. V. Vakhnina, A. A. Kuvshinov, N. M. Alexandrov, *Transformers at power facilities: tests, diagnostics, damageability, monitoring*. Moscow: Direct-Media,336 p. (2021)
9. V.I. Lazarev, I.V. Lazarev, *On the reason for the decrease in the forces of axial pressing of the windings of transformers in case of short-circuit*, Electrical engineering and electric power industry, Zaporozhye, No. 1, p.18 - 22 (2005)
10. A. Yu. Khrennikov, *Diagnostics of Electrical Equipment Faults and Power Overhead Transmission Line Condition by Monitoring Systems (Smart Grid): Short-Circuit Testing of Power Transformers*, Nova publishers, New York, USA, p. 165 (2016)
11. A. Yu. Khrennikov, A. A. Kuvshinov, I. A. Shkuropat, *Providing of reliable operation of electrical networks*, New York: NOVA PUBLISHERS, 296 p. (2019)
12. A. Yu. Khrennikov, English Original Reader for Technical Students. *Power transformers: short-circuit testing, monitoring systems (Smart Grid)*, Moscow, LITRES, 230 p. (2023)